CONF-961086--2

SAND--96-0708C
SAND96-0708C

Supercritical carbon dioxide solvent extraction from surface-micromachined micromechanical structures

C. W. Dyck*†, J. H. Smith*, S. L. Miller*, E. M. Russick**, C. L. J. Adkins**

*Integrated Micromechanics, Microsensors, and CMOS Technology Department
Sandia National Laboratories
MS-1078, P. O. Box 5800
Albuquerque, NM 87185-1078
†Under contract with the University of New Mexico, Center for High Technology Materials

**Encapsulants and Porous Materials Department
Sandia National Laboratories
MS-0367, P. O. Box 5800
Albuquerque, NM 87185-0367

ABSTRACT

Results are presented supporting the use of supercritical carbon dioxide ($SCCO_2$) drying to enhance the yield of surface-micromachined micromechanical devices following the final release etch. The equipment and extraction process of the $SCCO_2$ system are described, and results of successfully released cantilevered beams and microengines are presented. A new system capable of drying 6" wafers is also described.

Key words: Supercritical carbon dioxide, drying, surface micromachining, stiction, adhesion, release process, yield, microengines, cantilevers, solvent extraction.

2. REDUCING STICTION IN MICROMECHANICAL STRUCTURES

Thin film depositions, micron-scale patterning, and the capability to manufacture low-stress, thin films combine to make up surface-micromachined structures with features that are compliant and in close proximity to one another or the substrate. If one compliant feature comes into contact with an adjacent feature or the substrate, permanent adhesion between the surfaces can occur. This can happen at two different times. First, as structures dry following a sacrificial release etch, surface tension forces generated from diminishing liquid menisci trapped in the capillary-like spaces of adjacent surfaces can pull features into contact with each other or the substrate[1, 2]. Strong adhesive forces, referred to as stiction forces in micromechanics, can then cause devices to remain permanently stuck leading to unacceptably low yields after devices have dried. Surfaces can also come into contact with each other and remain stuck at a later time, such as during device operation, leading to reliability failures. The latter of the two failures is potentially the more costly.

Various mechanisms have been proposed to explain the causes of stiction[1-6]. The adhesion of two surfaces by solid impurities precipitating out of the rinse liquid has been reported as a cause[1, 2]. Results have been presented indicating that the dominant means of stiction between hydrophobic devices is through Van der Waals forces and that both Van der Waals forces and hydrogen bonding are responsible for stiction of hydrophilic surfaces[3]. Other work has indicated that adsorbed water on polysilicon surfaces is responsible[4, 5]. Electrostatic attraction has also been cited as a reason for stiction[6]. See references 2 and 3 for a review of stiction forces.

A great deal of work has been done to solve stiction failures in surface-micromachined structures[7-25]. Aside from maintaining an impurity-free release and rinse process, a number of techniques have been applied to increase both yield and long term reliability. Freeze-sublimation is a popular technique used to increase yield[7-11]. Using this method, devices are submersed in a solvent (or solvent mixture) and the then frozen. The liquid-vapor interface is avoided by sublimating the solidified solvent (or solvent mixture). Freeze-sublimation using a mixture of MeOH and H_2O was first used to dry micromechanical parts by Guckel, et al.[7]. Solvents such as cyclohexane[8, 9], t-butanol[10], and p-dichlorobenzol[11] have also been sublimated to dry devices. Other yield-enhancing techniques include the use of photoresist[12] or divinylbenzene[13] following the release etch. In the first, photoresist is applied, hardened, and then plasma ashed with an oxygen plasma to yield free standing structures. In the second, the monomer divinylbenzene is applied, polymerized with ultraviolet light, and then ashed with an oxygen plasma. Similarly, Mastrangelo and Soloka[14] have deposited the polymer parylene during processing and then ashed it with an oxygen plasma after the release etch.

The application of self-assembled monolayers (SAM's) is a very promising technique[2, 25, 26]. These are short or long chain molecules with a head group that reacts with hydrophilic silicon surfaces, and a tail group that increases the hydrophobicity of the silicon surface. This raises the H_2O contact angle of the surface above 90 degrees creating a repulsive meniscus force between adjacent surfaces that prevents them from contacting each other as they are drying. In addition to

This work was supported by the United States Department of Energy under Contract DE-AC04-94AL85000.

DISCLAIMER

enhancing the yield of post-release dried structures, SAM's provide long term device passivation to increase the reliability of surface-micromachined structures.

Physical roughening of contacting surfaces has been reported[17, 18]. Ammonium fluoride (NH_4F)[17] etches Si anisotropically at a rate of 60 - 120 Å/min (40% solution). <100> planes are attacked more quickly by this etchant. Therefore, in the random orientation of crystal planes such as that seen in polysilicon, the resulting etch treatment yields a roughened surface. Yee, et al.[18] have taken advantage of the variation in thermal oxide growth with doping to artificially create micromasking in the grain boundaries of phosphorous-doped polysilicon. In a two-step Reactive Ion Etch (RIE) process, a roughened surface is created. In both techniques the increased surface roughness decreases the contact area and distance between contacting surfaces. This reduces the stiction forces between the two surfaces which enhances both the yield and reliability of the structures.

Many other methods have also been used to eliminate stiction. Fedder and Howe[19] have used conductive supports for their compliant structures that were removed after the parts had been dried. Doped polysilicon beams anchored the devices preventing meniscus forces from initiating stiction. After the parts had been released and dried, the support beams were severed with high current pulses. Abe, et al.[20] have shown that incorporating the rinsing of devices with boiling liquids increases the yield of cantilever beams, possibly due to the decrease in surface tension and the increase in the vaporization rate of the liquids. Another yield-enhancing technique used Lorentz force deflection to free structures that had been stuck during drying[21]. Current pulses were applied to stuck devices that were immersed in a magnetic field acting perpendicular to the current flow creating a deflecting force perpendicular to the magnetic field orientation. In-use stiction been been decreased by passivating successfully released structures with silicon nitride (Si_3N_4).[8, 22] Stand-off bumps have also been fabricated on surfaces that have to come into contact with one another during device operation[23]. This has the same effect on stiction forces as surface roughening does. Abe and Reed[24] have recently designed tabs into their structures to increase the yeild. The tabs prevent liquid from drying in such a way that contact between adjacent surfaces from capillary effects is avoided.

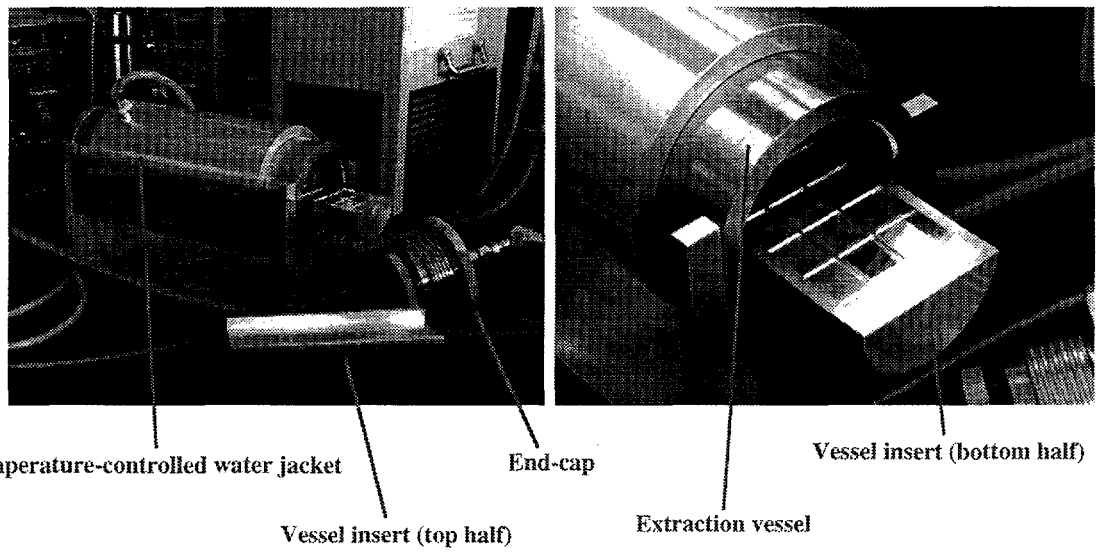

Figure 1: Pressure vessel and insert for $SCCO_2$ drying system.

The application of CO_2 solvent extraction to surface-micromachined structures was first demonstrated as an effective drying technique by the University of California at Berkeley[25]. Liquid CO_2 kept above the critical pressure (1073 psia) was used to dissolve and remove methanol (MeOH) from a pressure vessel containing micromachined structures. Once the MeOH was completely removed the temperature in the vessel was raised above the critical temperature of CO_2 (31.1C) and the vessel was vented. Since a liquid-vapor interface was not formed, capillary forces were unable to bring adjacent surfaces into contact with one another and stiction was not observed.

$SCCO_2$ solvent extraction has been used at our laboratories in other applications where surface tension effects have needed to be eliminated, as in the extraction of solvents from phase-separated polymer gels to produce microcellular foams[26], and in the extraction of solvents from silica aerogels[27]. This system operates slightly differently than the system used at Berkeley. CO_2 that is already in the supercritical region is used to dissolve and remove solvents from a pressure vessel, as opposed to the Berkeley system which uses liquid CO_2 to remove the solvents. $SCCO_2$ is similar to liquid CO_2 since it also dissolves methanol. Additionally, it possesses gas-like properties of diffusivity and viscosity that allow it to remove solvents from the narrow spaces between microstructure surfaces[28].

In this paper results are presented of successfully dried, singly clamped cantilever beams using both methanol and acetone. Results are also presented of successfully dried microengine devices. The solvent extraction system used to supercritically dry these devices is described. A new system capable of drying 6" wafers is also described. Results for this new system have not yet been obtained. The system is nearing completion of installation into our fabrication facility.

3. THE PRESENT $SCCO_2$ SYSTEM

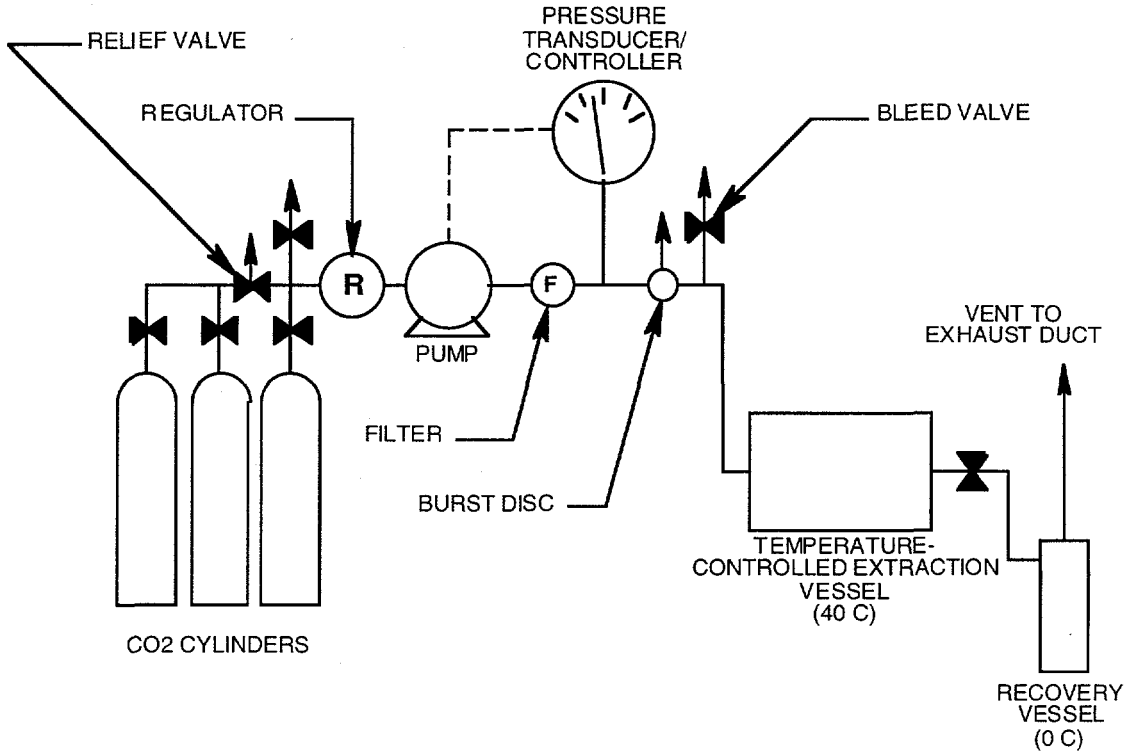

Figure 2: Basic elements of the $SCCO_2$ solvent extraction system.

A rough schematic of the $SCCO_2$ system is shown in Figure 2. The extraction vessel was manufactured by Thar Designs, Inc. The vessel volume is 1 liter. It has an inner diameter of 3" and an inner height of 8". The vessel sits on its side during the extraction process (Figure 1). The volume of the vessel was reduced to approximately 190 mL by inserting a two-piece cylindrical plug. This decreased the solvent displacement time by $SCCO_2$. A tray was machined into the bottom half of the plug. The floor of the tray had a grid machined into it that fit 27 1/2" x 1/2" dies. The grid of squares was interconnected to facilitate a quicker displacement time when larger sample were dried in the vessel. The interconnected grid prevented solvents from being trapped under the larger samples. The vessel is constructed of 17-4 pH stainless steel and has a maximum allowable working pressure of 10,000 psi. The temperature of the vessel is controlled by a circulating bath that heats the vessel by means of a heating jacket (Thar Designs, Inc.) placed around the outside of the vessel.

The pressure control system consists of a pneumatic pump controlled by an Autoclave modular pressure controller with digital readout. CO_2 is delivered to the vessel, through the pneumatic pump (Gas Booster, model AGD-30, Haskel Corp.), from 3 size 1A technical grade CO_2 cylinders. A regulator is placed between the cylinders and the pump so CO_2 gas flow can be increased slowly at the beginning of each run. The CO_2 flows from the pump to the vessel through a pressure monitor placed adjacent to the vessel opening. The pressure monitor is connected to the controller which in turn controls the pneumatic pump. To prevent particle contamination from any hardware upstream from the vessel, a 0.5 micron sintered stainless steel filter was placed near the input to the pressure vessel.

The exhaust system consists of a recovery vessel (cyclone separator), a circulating bath, heating tape, and a temperature controller. $SCCO_2$ and solvent flow out of the vessel into a 500 mL separator (Thar Designs, Inc.). The separator has an input opening on its side, an output at the top, and an output connected to a valve at the bottom. It is cooled to 0°C with an exchanger (Thar designs, Inc.) that is connected to a circulating bath. The bottom output of the separator is used to drain condensed solvent from the displacement process and the top outlet is used to vent the carbon dioxide into a stack along with any uncondensed solvent. There is a metering valve between the vessel output and the cyclone separator input to slowly

increase the flow of CO_2 and MeOH out of the vessel. This valve is wrapped in heating tape to prevent icing in the tubing during CO_2 expansion. All tubing for the system is T-316 stainless steel, 1/4" O.D.

4. FABRICATION

An array of cantilever beams were fabricated using a single-level, surface-micromachining process. The cantilevers were arranged in 2 μm increments from 10 μm to 100 μm, and in 5 μm increments from 100 μm to 500 μm. Beam widths were 10 μm and 20 μm. 2 μm of silicon dioxide (oxide) was deposited on the substrate and then densified in a dry oxygen ambient. The oxide was deposited by low pressure chemical vapor deposition (LPCVD) by reacting tetraethylorthosilane with oxygen. Approximately 2.25 μm of microcrystalline (or amorphous) polysilicon was deposited by LPCVD over the oxide by the thermal decomposition of silane gas. A second layer of oxide was deposited on top of the polysilicon to serve as a hard mask for patterning the cantilevers. The polysilicon and oxide layers were annealed at high temperature in a nitrogen ambient since this has been shown to decrease, however not completely eliminate stress in the polysilicon structural material[12]. The oxide mask was anisotropically etched by reactive ion etching (RIE) with a CHF_3/C_2F_6 chemistry using a photoresist mask. The polysilicon material was etched by RIE in a HBr/Cl chemistry. The cantilevers were released in a 1:1 $HF:H_2O$ solution for 30 minutes. This was a sufficient amount of time to release the beams while not detaching the cantilever bases from the substrate.

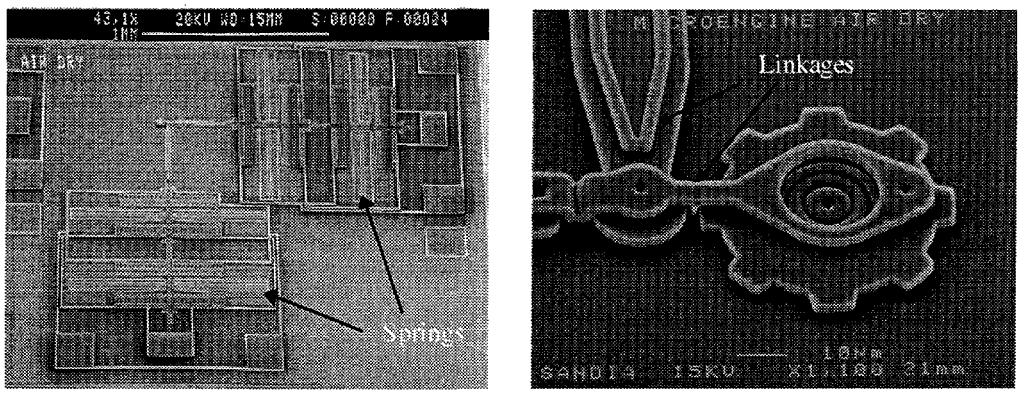

(a) **(b)**

Figure 3: Complete microengine (a) and (b) close-up of gear and linkages.

Fabrication of the microengines has been described previously[29]. The engines were constructed using an extension of the single-level surface micromachining process. A sample microengine is shown in Figure 3a. The release time for these devices was 90 minutes in a 1:1 $HF:H_2O$ solution. It is evident from Figure 3 that there are compliant beams and movable parts that are susceptible to stiction following the final rinse and dry, and to stiction during the actual operation of the engine. Two trouble spots in particular are (1) the springs connecting the comb drive shuttle to the substrate (the springs appear as thin, white beams in Figure 3a), and (2) the gear (Figure 3b). The spring dimensions for the microengines that were tested here are 700 μm in length, 2 μm in height, and 2 μm in width. They are suspended at a distance of roughly 2 μm from the substrate which makes susceptible to capillary forces during drying. The freedom of movement in the gear, and in the linkage that connects the gear to the comb drive shuttle allow the gear to touch the substrate and the central hub. As a consequence, capillary forces during drying can easily initiate stiction between either the gear and the hub or between the gear and the substrate. The gear area is also susceptible to in-use stiction during its operation.

5. EXPERIMENTAL

Cantilevers and engines were dried using the following sequence of steps. After the sacrificial oxide wet etch the parts were rinsed in deionized (DI) H_2O for 30 minutes. Devices were then transferred into containers of pure solvent (MeOH or acetone). Before the transfer solvent was added to the rinse containers so the engines and cantilevers would not de-wet. Solvent was poured into the pressure vessel tray and the devices were transferred from the container full of solvent into the tray. Approximately 20 mL of solvent was sufficient to completely cover all of the devices in the tray and allow for evaporation that occurred between the transfer time and the introduction of $SCCO_2$ into the vessel. The tray was placed into the pressure vessel and the vessel was sealed.

The output metering valve and the input regulator valve were initially shut after the parts had been loaded into the vessel. The vessel pressure was increased slowly to avoid destroying the micromechanical devices. The valves connecting the CO_2 containers to the regulator were opened first. Then the regulator valve was slowly opened until the vessel pressure

reached approximately 780 psia, the ambient CO_2 vapor pressure in the container. This took about 5 minutes and was done manually. Next the pressure controller was set at the operating pressure (above the critical pressure for CO_2) and the pneumatic pump was turned on. Again, the regulator valve was used to slowly increase the pressure in the vessel. This pressure increase took another 5 minutes. When the vessel reached the operating pressure, the outlet metering valve was slowly opened (another 5 minutes) to start the $SCCO_2$ flow. The $SCCO_2$ flow rate was measured to be about 30 g/min by taking mass measurements of the CO_2 cylinders before and after each run. After the solvent in the vessel had been displaced, the output metering valve was closed. The pneumatic pump was also shut off, and the CO_2 container valve was closed. The vessel was purged slowly with the output metering valve (about 5 minutes) and the devices were removed from the vessel.

In our previous work a variety of surface-micromachined devices were successfully dried[30]. It was found that $SCCO_2$ densities close to or greater than the MeOH density resulted in faster extraction times. For this work the microengines and cantilevers were supercritically dried at 2300 psia and 35°C, a $SCCO_2$ density equal to the density of MeOH (0.79 g/mL). Approximate extraction times for these conditions were between 30 minutes and 45 minutes. To account for any variation, the extraction time of 60 minutes was used. The total run time was the sum of solvent extraction time, the pressurization time, and the depressurization time. Ramping the pressure up and down took approximately 20 minutes so the total drying time was 80 minutes.

Thirteen cantilever arrays were supercritically dried in two runs using MeOH as the solvent. One run contained a cleaved sample with 8 cantilever arrays and the other run contained a cleaved sample (from the same wafer) with 5 cantilever arrays. The cantilevers were viewed optically and the first cantilever length in each array that was stuck was recorded (this has been termed the *detachment length* in other work[3, 5]). The detachment length for all 13 of the arrays was averaged and entered into Table 1. This was done for both the 10 μm wide cantilevers and the 20 μm wide cantilevers.

Three cleaved samples containing microengine dies were supercritically dried in two runs using MeOH as the solvent. All 3 pieces originated from the same wafer. Each microengine die contained 4 different engine types. The type of engine shown in Figure 3 was tested on each die for consistency. During the first run one piece (sample 1) was dried that consisted of 32 complete die. Thirty out of 32 microengines were tested at the probe station within 3 hours of the drying process. One of the untested die had been damaged during the release and dry process and one die had been incompletely processed (edge-of-wafer die). *Sticking yield* data was recorded for this sample as the percentage of free parts and entered into Table 2. The sticking yield data did not include properly functioning devices. This figure only took into account whether the devices were free or not. A gear that displayed at least partial rotation and had all eight springs free was considered a free device. A gear that showed either a stuck gear or had one or more immobile springs was considered a stuck device. The microengines from this sample were also tested 4 subsequent times over a 10 day period. The average sticking yield was plotted versus time in Figure 4. Two cleaved samples (2 and 3) were dried during the second run (again using MeOH as the solvent). Sample 2 contained 21 complete die and the sample 3 contained 4 complete die. Seventeen out of 21 microengines were tested on sample 2. Two of the engines not tested had been damaged during the release and dry process and 2 of the engines had been incompletely processed at the edge of the wafer. All 4 engines were tested for sticking yield on sample 3. Both of these samples were tested within 3 hours of the supercritical drying process. Sitcking yield data was entered into Table 2.

Drying Method	# of Arrays	Avg. Detachment Length (μm)	
		Thin Array	Thick Array
Air-Dry (Control)	12	95.8	94.4
$SCCO_2$ - MeOH	13	>500	>500
$SCCO_2$ - Acetone	4	>500	>500

Table 1: Cantilever detachment lengths for controls and supercritically dried samples.

In addition to extracting MeOH, acetone was extracted with $SCCO_2$. One cleaved sample with 24 complete microengine die and one cleaved sample with 4 cantilever arrays were supercritically dried in a single run using the same pressure, temperature, and time as the previous runs. The cantilevers and microengines were examined using the same techniques as in the previous runs. Twenty three out the 24 of the microengines were tested (1 was damaged during the release and dry process). Sticking yield data was calculated for the microengines (Table 2) and the average detachment length was recorded for the cantilever arrays (Table 1).

Drying Method	# of Engines	Sticking yield (%)
Air-Dry (Control)	35	0
$SCCO_2$ - MeOH	57	78.4
$SCCO_2$ - Acetone	23	78.3

Table 2: Microengine yield for controls and supercritically dried samples.

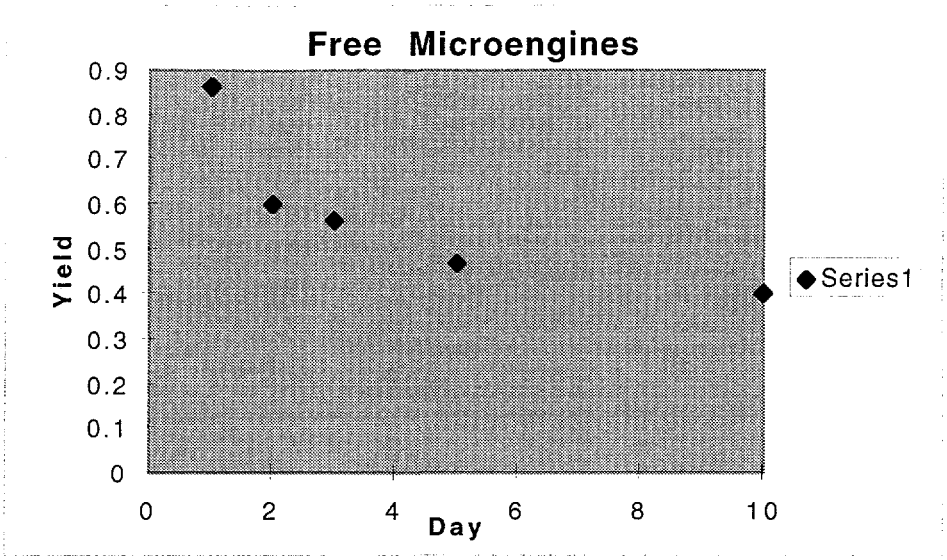

Figure 4: Sticking yield vs. time for microengines (sample 1).

A control sample of 35 microengines and 12 cantilevers were also dried for comparison. These samples were released and rinsed in DI H_2O under the same conditions that were described earlier. Since these devices were dried merely to provide a comparison with the supercritically dried devices the rinsing and drying times were not tightly controlled. The cantilevers were rinsed for 30 minutes and then extracted from the rinse solution and placed on the counter (air dry). The polysilicon surfaces were still seen to be hydrophobic. The cantilever beams were viewed optically after having been out of liquid for 30 minutes. The average detachment length for the 12 cantilever arrays was calculated and was entered in Table 1. Two cleaved samples of microengines were rinsed in DI H_2O for 90 minutes and then soaked in the same container until they were hydrophilic. Both samples contained 18 microengine die. All 18 die were tested on the first sample and 17 out of 18 were tested on the second sample. One die was damaged on the second sample by the release and dry process. The microengines were tested at the probe station within a couple of hours of being extracted from the rinse container. Sticking yield data for the microengine control samples was entered into Table 2.

To assess the overall impact of $SCCO_2$ drying on the complete back end of the process (from the release through packaging), 252 microengines were released, supercritically dried, and then packaged. No additional surface treatments were applied to these devices to enhance their reliability. The devices were packaged and tested in 40-pin dips 5 days after drying. They were tested 2 more times in one week intervals. During the time interval between drying and packaging the devices were stored in closed plastic packages in ambient conditions of 40% humidity and 23°C. A new set of yield and failure criteria were defined for the packaged devices. Only fully functioning devices were counted as yielding devices (*functional yield*). A fully functioning device was one that passed the sticking yield criteria and displayed a fully rotational gear. Failures were categorized as being caused by sticking, or by other miscellaneous reasons. Sticking failures were determined by prodding various parts on the microengine with a manually operated probe tip. Damage was visible (broken springs, broken comb teeth on the comb drive actuator, detached gear, etc...) under the microscope. Miscellaneous failures such as shorts or interference caused by debris could be seen under the microscope or by using a digital multimeter. Functional yield data for the microengines is shown in Table 3.

Engine Category	Functional yield (%)		
	1st Test	Week 1	Week 2
Functioning	32	24	24
Stuck	36	37	37
Misc. Failure	32	39	39

Table 3: Microengine functional yield of packaged parts.

6. RESULTS & DISCUSSION

The average detachment lengths of the 10 μm wide and 20 μm wide cantilever controls that were dried in air were 94.4 μm and 95.8 μm, respectively (Table 1). The detachment lengths had similar magnitudes, as they should have had, since the detachment length of cantilevers has been shown to be independent of the cantilever width[5]. An SEM photo of one air dried array of cantilevers is shown in Figure 4a. The detachment length of this array (for the 10 μm wide cantilevers) was

100 μm. Using supercritical drying with both MeOH and acetone, the detachment length increased beyond 500 μm for both types of cantilever arrays. This represented a decrease in the adhesion energy of greater than 3 orders of magnitude (using the equations derived in reference 5, neglecting film stress and assuming the beams are rigid near the anchor). Unfortunately, longer cantilevers were not available for drying so our results could not be compared to Mulhern's work[25]. A SEM photo of one of the supercritically dried arrays is shown in Figure 4b. The longest cantilever appears stuck in the photo. This was not caused by the supercritical drying since all of the arrays were viewed optically and verified to be 100% free before the SEM photos were taken. This has been attributed to electrostatic interactions between the cantilever and the substrate caused during SEM observation. In the past it has been common to see cantilevers being drawn into contact with the substrate during SEM observation.

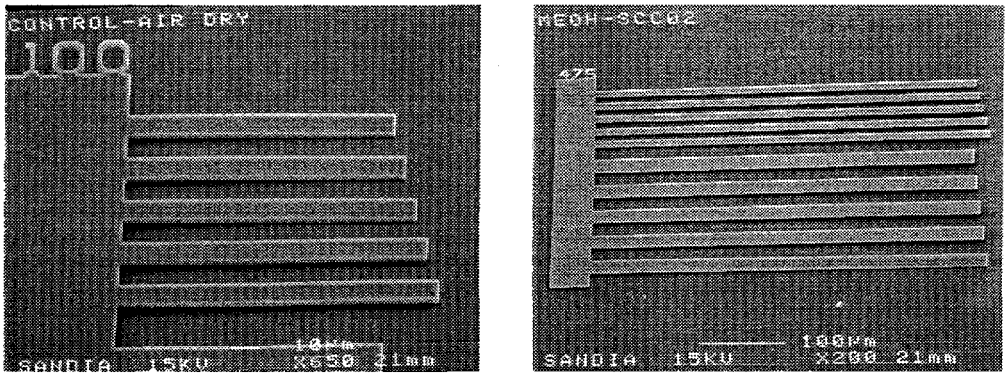

(a) (b)

Figure 4: (a) Stuck cantilevers (controls) and (b) supercritically dried cantilevers. Electrostatic attraction from SEM viewing caused the 500 μm cantilever to stick.

The sticking yield for the microengines dried in air (Table 2) was 0%. All of these engines either failed to show any gear rotation or had at least one stuck spring. This was consistent with past results obtained from testing at our facility. Typically, microengines that have not undergone any sort of anti-stiction treatment during the release and dry process have exhibited 0 - 8% functionality[31]. As it was mentioned earlier one of the two main areas of sticking on the microengine has been the springs. Manually prodding the springs with a probe tip and SEM photos of some of the stuck microengines confirmed that the springs had caused some of the stiction failures. Figure 5a shows SEM photos of a stuck spring.

The percentage of unstuck microengines increased to about 78% using $SCCO_2$ drying (Table 2). Eight out of the 11 failures from the 3 samples that were dried by extracting MeOH from the vessel occurred at the edges of the cleaved pieces. This was a good indicator that some of the edge dies on these samples could have become de-wetted during one of the bath transfers which caused stiction in the microengines. The cause of the other failures that occurred during the MeOH extraction drying process needs further investigation. Only 1 out of 5 failures from the engines that were dried by extracting acetone from the vessel was located on an edge die. The same conclusion that was made for the engines dried by extracting MeOH probably cannot be made here. It is possible that certain areas on the dies became de-wetted by evaporation of the acetone during the transfer from the acetone bath to the vessel, since the vapor pressure of acetone is higher than the vapor pressure of MeOH. Again, the failures here need further investigation.

The plot in Figure 3 shows a rapid decrease in the sticking yield of sample 1 that levels off after about 5 days. An increased number of stuck springs and gears was observed over this 10-day period which resulted in some of the decreased sticking yield. Physical damage that may have occurred on these devices from handling was not observed, and therefore the increased number of failures was not attributed to this.

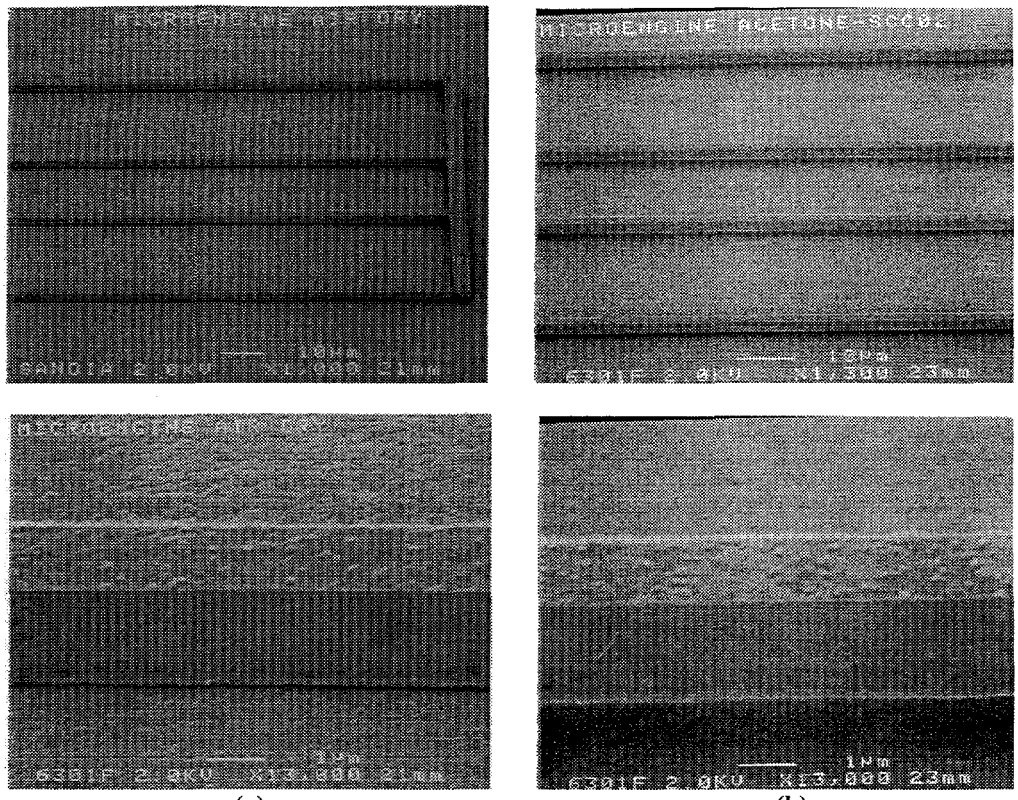

(a) (b)

Figure 5: Microengine spring SEM's showing (a) air dried controls, (b) supercritically dried springs (using acetone).

Results listed in Table 3 show that 32% of the microengines that were packaged and tested (Test 1) 5 days after they had been dried were functioning correctly. After 2 more tests in 1 week intervals, the percent of functioning devices dropped to 24%. The percentage of stuck microengines was 36% and increased to 37% over the next 2 weeks. The small change in failures caused by sticking over the two week period is consistent with the plot of the sticking yield in Figure 3. Figure 3 showed a leveling off of the sticking yield after 5 days. The packaging process for this experiment lasted about 5 days from the time of supercritical drying. After the devices had been packaged the functional yield was stable over the two-week period of the test. Miscellaneous failures increased from 32% to 39%. It turned out that most of these were traced to a shorting problem with the engines.

The results from Table 3 were probably the most impressive in showing the impact of $SCCO_2$ drying on the microengine yield. The results from Table 1 show that the microengine sticking yield for devices dried in air was 0%, and as it was mentioned earlier past accounts have indicated a functional yield value over the interval of 0% - 8%. By using supercritical drying the functional yield was increased by a factor of 3. Since a large percentage of devices were free after drying, other failure mechanisms in the microengines were able to be investigated. An electrical shorting problem was discovered that might otherwise have been convoluted by the stiction failures.

7. CONCLUSIONS

$SCCO_2$ drying was demonstrated to be effective in enhancing the yield of surface-micromachined devices. Both MeOH and acetone were extracted by $SCCO_2$ during the drying process. The detachment length of cantilever beams was increased beyond 500 μm, representing a greater than 3 orders of magnitude decrease in adhesion energy. The sticking yield of microengines increased from 0% to 78%. In a test of 252 packaged microengines, the functional yield was increased by a factor of three to 24%.

8. APPENDIX: THE NEW $SCCO_2$ DRYING SYSTEM

A new $SCCO_2$ drying system has been designed and is being installed into our fabrication facility (Figure 6). The system will be capable of drying 6" wafers. It operates on the same principle as the Berkeley system, using liquid CO2 to displace solvent in the pressure vessel. This section describes the new system.

The vessel is constructed of T-316 stainless steel. It is a slight modification of High Pressure Equipment Company's (HiP) BC series bolted closure vessels. The vessel inner diameter is 7.75" and its inner height is 4" giving it a total volume of close to 3 liters. The maximum operating pressure of the vessel is 3000 psi at 343C. The vessel capacity has been decreased by an aluminum plug and a teflon tray that is capable of holding a single 6" wafer. The tray has been designed so that another tray can be stacked on top of it. Potentially, as many as four 6" wafers could be dried in a single run. A drain valve (HiP) has been connected to the bottom of the vessel to serve as the output for the liquid CO_2 and the solvent.

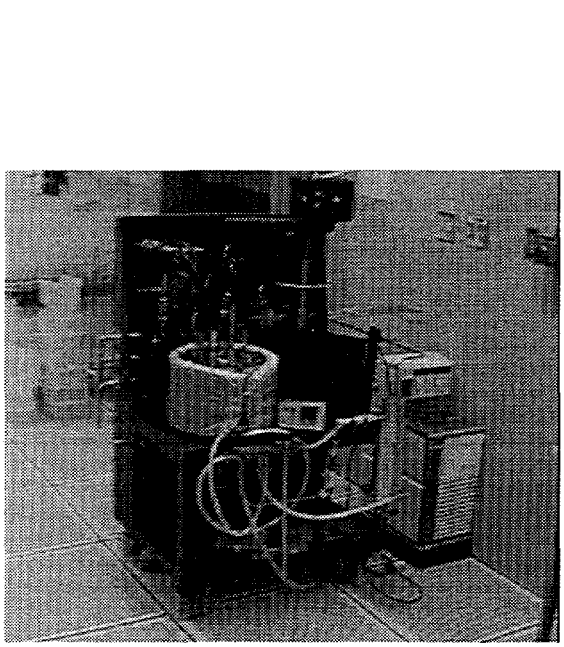

(a)

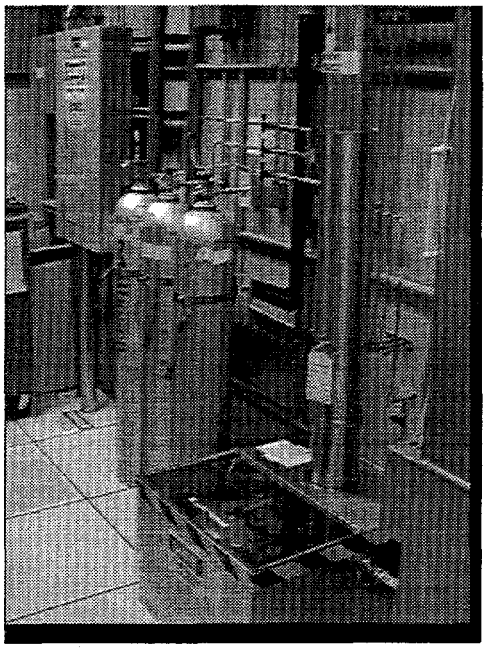

(b)

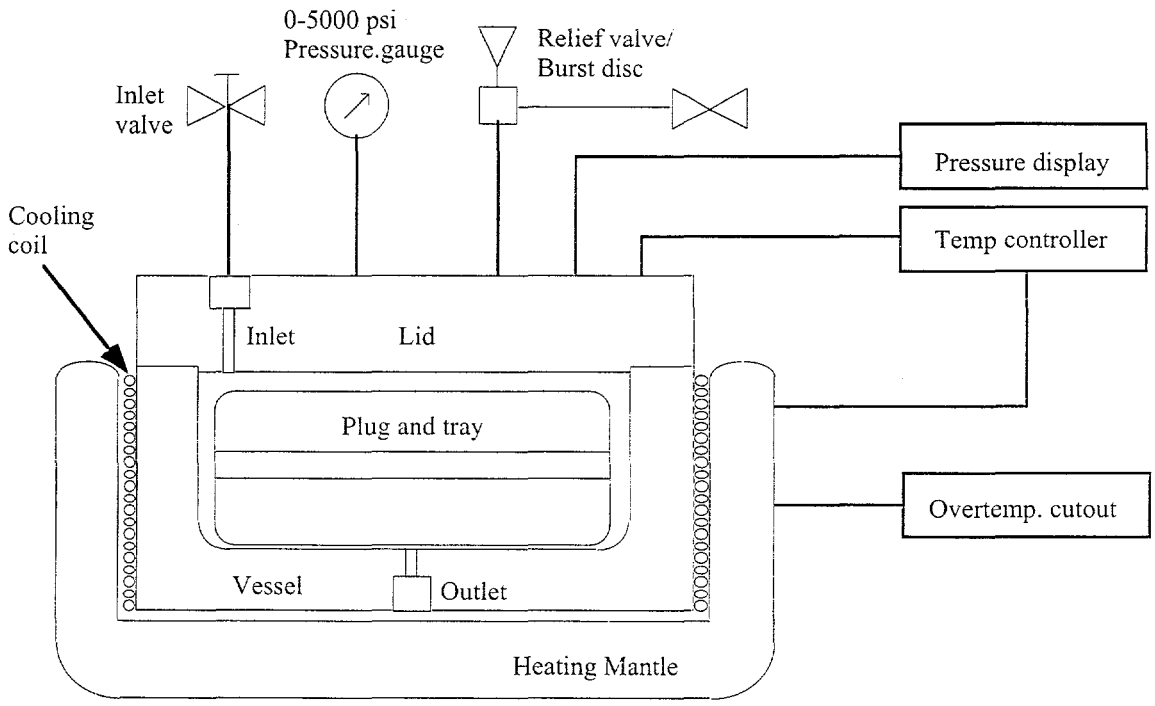

(c)

Figure 6: The new $SCCO_2$ dyring system: (a) back of system showing vessel, heating mantle and circulating bath, (b) CO_2 stored in the adjacent chase, and (c) sketch of vessel and attachments.

The lid is sealed with a teflon O-ring and fastened with 12 threaded bolts requiring 100 ft-lb of torque each. The lid contains a number of attachments for an inlet valve, temperature and pressure monitoring, and a pressure relief system (see Figure 6c for a block diagram of the vessel and attachments). The inlet valve is a standard open-shut valve (HiP). It has been placed away from the center of the lid to prevent liquid CO_2 from entering the vessel directly over the wafers. Two other inlets may also be used to flow CO_2 into the system. They, too, have been placed away from the center of the lid. A 1/16" diameter J-type thermocouple (Omega) has been connected to the lid to monitor the temperature during the drying process. It is connected to the lid with a threaded bolt and is in direct contact with the fluids in the vessel. Two attachments have been made to the lid for pressure monitoring. One is for a mechanical gauge mounted on the front side of the system (not visible in Figure 6a). The second is for a pressure transducer that is connected to a digital readout, in a 12" x 10" x 6" box, mounted on the front side of the system. An analog output (0-5 Volts) will be used to record pressure readings from the interior of the vessel. An attachment is also made from the lid to a 3000 psi relief valve and a 5000 psi burst disc.

The pressure vessel is wrapped in a flexible heating mantle (Glas-Col). The mantle is controlled by a PID controller that is mounted next to the pressure monitor. Temperature is monitored by the thermocouple attached to the lid of the vessel. The PID controller is also equipped with a 0-5 Volt analog output. A copper cooling coil has been placed between the heating mantle and the outer wall of the pressure vessel. Chilled liquid will be circulated through the coil between runs in order to cool the system down below the critical temperature of CO_2. A 7 liter circulating bath (Fisher Scientific) controls the temperature of the chilled liquid.

Liquid CO_2 back-filled with a helium head to 1800 psi (Trigas, New Mexico) is stored in 3 containers in the neighboring chase (Figure 6b). Each CO_2 container has its own line and an open-shut valve connected to it. The three CO_2 lines merge into a single line in the chase. This line runs into the fabrication area and through a metering valve. The metering valve controls the flow into the pressure vessel so that micromechanical devices are not damaged as the pressure is being ramped up. Exhaust from the vessel emerges from the bottom drain valve and runs through a second metering valve to a chilled separator. The separator is a 500 mL vessel (Thar Designs) encased in a cooling jacket (Thar Designs). The cooling jacket is chilled by liquid from the same circulating bath that is used to cool the vessel between runs. Two switching valves are used to control the direction of flow from the circulating bath. During solvent displacement, chilled water is diverted to the separator in order to separate the solvent from the liquid CO_2. The solvent is removed from the separator between runs by a drain valve. The switching valves divert chilled liquid from the circulating bath to the cooling coil around the vessel to bring it back below the critical temperature of CO_2 between runs.

9. ACKNOWLEDGEMENTS

The authors wish to thank the entire staff of operators and engineers and Microelectronics Development Lab, without whom none of the micromechanical devices could have been manufactured. Special thanks go to Jeff Sniegowski for providing microengines and cantilevers, to Pat Shea for the SEM work in this paper, and to the Device Testing and Modeling Group for their assistance in testing. The authors would also like to thank Greg Mulhern and Mike Houston from the Berkeley Sensors & Actuator Center at the University of California at Berkeley for their consultation in the design of the new $SCCO_2$ drying system.

10. REFERENCES

1. H. Guckel and D. W. Burns, "Fabrication of micromechanical devices from polysilicon films with smooth surfaces," *Sensors and Actuators A*, 20, pp. 117-122, 1989.

2. R. L. Alley, G. J. Cuan, R. T. Howe, and K. Komvopoulos, "The effect of release-etch processing on surface microstructure stiction," *IEEE Solid-State Sensors and Actuators Workshop*, Hilton Head, SC, pp. 202-207, 1992.

3. R. Legtenberg, H. A. C. Tilmans, J. Elders, and M. Elwenspoek, "Stiction of surface micromachined structures after rinsing and drying: model and investigation of adhesion mechanisms," *Sensors and Actuators A*, 43, pp. 230-238, 1994.

4. P. R. Sheeper, J. R. Voorthuyzen, and P. Bergveld, "Surface forces in micromachined structures," *Micromechanics Europe*, pp. 26-31, 1990.

5. C. H. Mastrangelo and C. H. Hsu, "A simple experimental technique for the measurement of the work of adhesion of microstructures," *IEEE Solid-State Sensors and Actuators Workshop*, Hilton Head, SC, pp. 208-212, 1992.

6. C. Linder, E. Zimmerman, and N. F. de Rooy, "Capacitive polysilicon resonator with MOS detection circuit," *Sensors and Actuators A*, 25-27, pp. 591-595, 1991.

7. H. Guckel, J. J. Sniegowski, and T. R. Christenson, "Fabrication of micromechanical devices from polysilicon films with smooth surfaces," *Sensors and Actuators*, 20, pp. 117-122, 1989.

8. J. J. Sniegowski, "Design and fabrication of the polysilicon resonating beam force transducer," phD thesis, Department of Nuclear Engineering and Engineering Physics, University of Wisconsin, pp. 87-103, 1991.

9. R. Legtenberg and H. A. C. Tilmans, "Electrostatically driven vacuum-encapsulated polysilicon resonators. Part I. Design and fabrication," *Sensors and Actuators A*, 45, pp. 57-66, 1994.

10. N. Takeshima, K. J. Gabriel, M. Ozaki, J. Takahashi, H. Horiguchi, H. Fujita, "Electrostatic Parallelogram Actuators," *International Conference on Solid-State Sensors and Actuators (Transducers '91)*, pp. 63-66, 1991.

11. D. Kobayashi, T. Hirano, T. Furuhata, H. Fujita, "An integrated lateral tunneling unit," *Proc. IEEE Micro Electro Mechanical Systems (MEMS '92)*, pp. 214-219, 1992.

12. M. Orpana and A. O. Korhonen, "Control of residual stress of polysilicon thin films by heavy doping in surface micromachining," *International Conference on Solid-State Sensors and Actuators (Transducers '91)*, pp. 266 - 269, 1991.

13. F. Kozlowski, N. Lindmair, Th. Scheiter, C. Heirold, and W. Lang, "A novel method to avoid sticking of surface micromachined structures," *International Conference on Solid-State Sensors and Actuators (Transducers '95)*, pp. 220-223, 1995.

14. C. H. Mastrangelo and G. S. Saloka, "A dry-release method based on polymer columns for microstructure fabrication," *Proc. IEEE Micro Electro Mechanical Systems (MEMS '93)*, pp. 77-81, 1993.

15. K. Deng, R. J. Collins, M. Mehregany, and C. N. Sukenik, "Performance impact of monolayer coating of polysilicon micromotors," *Proc. IEEE Micro Electro Mechanical Systems (MEMS '95)* , pp. 368-373, 1995.

16. M. R. Houston, R. Maboudian, and R. T. Howe, "Self-assembled monolayer films as durable anti-stiction coatings for polysilicon microstructures," *IEEE Solid-State Sensors and Actuators Workshop*, Hilton Head, SC, pp. 42-47, 1996.

17. M. R. Houston, R. Maboudian, and R. T. Howe, "Ammonium fluoride anti-stiction treatments for polysilicon microstructures," *International Conference on Solid-State Sensors and Actuators (Transducers '95)* , pg. 210-213, 1995.

18. Y. Yee, K. Chun, and J. D. Lee, "Polysilicon surface modification technique to reduce sticking of microstructures," *International Conference on Solid-State Sensors and Actuators (Transducers '95)*, pp. 206-209, 1995.

19. G. K. Fedder and R. T. Howe, "Thermal assembly of polysilicon microstructures," *Proc. IEEE Micro Electro Mechanical Systems (MEMS '89)*, pp. 63-68.

20. T. Abe, W. C. Messner, and M. L. Reed, "Effects of elevated temperature treatments in microstructure release procedures," *IEEE Journal of Micro Electro Mechanical Systems*, vol. 2, no. 2, pp. 65-75, 1995.

21. B. P. Gogoi and C. H. Mastrangelo, "Adhesion release and yield enhancement of microstructures using pulsed lorentz forces," *IEEE Journal of Micro Electro Mechanical Systems*, vol. 4, no. 4, pp. 185-192, 1995.

22. L. S. Tavrow, S. F. Bart, J. H. Lang, "Operational characteristics of microfabricated electric motors," *Sensors and Actuators A*, 35, pp. 33-44, 1992.

23. W. C. Tang, T. -C. H. Nguyen, and R. T. Howe, "Laterally driven polysilicon resonant microstructures," *Proc. IEEE Micro Electro Mechanical Systems (MEMS '89)*, pp. 63-68, 1989.

24. T. Abe and M. L. Reed, "Control of liquid bridging induced stiction of micromechanical structures," *J. Micromech. Microeng.*, 6, pp. 213-217, 1996.

25. G. T. Mulhern, D. S. Soane, R. T. Howe, "supercritical carbon dioxide drying of microstructures," *International Conference on Solid-State Sensors and Actuators (Transducers '93)*, pp. 296-299, 1993.

26. D. A. Loy, G. M. Jamison, B. M. Baugher, E. M. Russick, R. A. Assink, S. Prabakar, and K. J. Shea, *J. Non-Crystalline Solids*, 186, pp. 44-53, 1995.

27. E. M. Russick, and J. H. Aubert, "Supercritical carbon dioxide extraction of gel-derived polymer foams," *Sandia National Laboratories Technical Report SAND92-1122*, 1992.

28. McHugh and V. J. Krukonis, *Supercritical Fluid Extraction: Practise and Principles*, Butterworths, Boston, 1986.

29. E. J. Garcia and J. J. Sniegowski, "Surface micromachined microengine," *Sensors and Actuators A*, 48, pp. 203-214, 1995.

30. E. M. Russick, C. L. J. Adkins, C. W. Dyck, Supercritical carbon dioxide extraction of solvent from micromachined structures, *Proc. Spring American Chemical Society Conf.*, New Orleans, LA, 1996, to be published.

31. Ken Hughes, Test engineer at the Microelectronics Development Labs, Sandia National Labs, Org. 1325, private communication.